# Substrate Integrated Waveguide Single-Pole Dual-Double-Throw (SPDDT) Switch for K-Band Applications

Deisy Formiga Mamedes#1, Jens Bornemann#2
#Department of Electrical and Computer Engineering, University of Victoria
Victoria, BC, V8W 2Y2, Canada
1 mamedes@uvic.ca
2 j.bornemann@ieee.org

2021 IEEE Asia-Pacific Conference on Applied Electromagnetics (APACE) | 978-1-6654-2827-9/21/$31.00 ©2021 IEEE | DOI: 10.1109/APACE53143.2021.9760636

***Abstract* — A substrate integrated waveguide (SIW) single-pole dual-double-throw (SPDDT) switch for K-band multiple beam antenna feeds and/or 5G applications is presented. The design can be straightforwardly integrated with other SIW or planar circuitry. The SPDDT switch is based on a coupler that is reconfigured to control electromagnetic wave propagation to different sets of output ports. Results demonstrate that the proposed switch has an isolation better than 15 dB from 18 to 27.4 GHz.**

**Index Terms — coupler, K-band, single-pole dual-double-throw, substrate integrated waveguide, switch**

## I. Introduction

Due to the growth of wireless communication applications, modern telecommunication systems require the use of frequency bands in the millimeter-wave (mm-wave) range [1, 2]. For such applications, it is important to develop planar technologies that can be readily incorporated in these systems.

Substrate Integrated Waveguide (SIW) technology has been demonstrated to be a viable alternative to conventional waveguide and microstrip circuitry, being suitable for commercial mm-wave systems [3]. An SIW consists of two rows of via holes placed as side walls in a parallel plate waveguide filled with a dielectric material [4]. The advantages of this technology include easy integration with planar devices, compact size, low-cost, and low-profile [5, 6]. SIW technology has been implemented in antennas, filters, switches, etc., and SIW switch designs have been reported based on mechanical [7], ferrite-loaded [8], and electronic [9] switch operation.

Therefore, this paper focuses on an SIW single-pole dual-double-throw switch design for K-band multiple beam antenna and/or 5G applications. It is based on an SIW coupler with added inductive posts and connected PIN diodes. By employing the on- and off-states of the PIN diodes, the electromagnetic waves can be directed to different sets of coupler output ports. This application is suited for feed networks of multiple beam antennas and/or for 5G applications.

## II. Design

### A. Single-Pole Single-Throw Switch

Initially, a single-pole-single-throw (SPST) switch is designed using SIW technology as shown in Fig. 1. First, an all-dielectric waveguide technology is designed by determining the equivalent waveguide width $W_{eq}$ using (1) from [4]

$$W_{eq} = \frac{c}{2 f_c \sqrt{\varepsilon_r}} \quad (1)$$

where $c$ is the speed of light in free space, $f_c$ the cutoff frequency, and $\varepsilon_r$ the relative permittivity of the substrate.

The translation to the respective SIW width is obtained by (2) from [4]

$$a_{SIW} = W_{eq} + p\left(0.766 e^{0.4482 d/p} - 1.176 e^{-1.214 d/p}\right) \quad (2)$$

for given diameter $d$ and via pitch $p$.

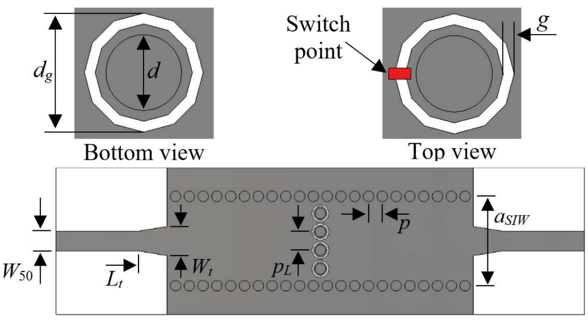


Fig. 1. SIW SPST switch parameters with bottom and top views around the inductive posts.

The microstrip-to-SIW transitions are designed according to [10]. For a 50-Ω microstrip line with width of $W_{50}$, the transition width $W_t$ and length $L_t$ are calculated using (3) and (4), respectively

$$\frac{1}{h\left[\dfrac{W_t}{h} + 1.393 + 0.667 \ln\left(\dfrac{W_t}{h} + 1.444\right)\right]} = \frac{4.38}{W_{eq}} e^{-0.627 \varepsilon_r / \varepsilon_e} \quad (3)$$

and

$$L_t = \frac{\lambda_g}{4} \quad (4)$$

where $h$ is the height of the substrate and

$$\lambda_g = \frac{c}{f\sqrt{\varepsilon_r}} \quad (5)$$

$$\varepsilon_e = \frac{\varepsilon_r + 1}{2} + \frac{\varepsilon_r - 1}{\sqrt{1 + 12\dfrac{h}{W_t}}} \quad (6)$$

For the final configuration, four inductive posts are placed in the middle of the SIW, as shown in Fig. 1, with spacing of $p_L$. The number of posts depends on the width of the SIW. Switch points are created by circular slots surrounding each inductive post on the top and bottom of the structure with diameter $d_g$ and gap $g$, and a PIN diode is added on the top plane for switching (Fig. 1). Note that diode biasing is provided between the SIW ground plane (top and bottom connected by via holes) and the insulated post at the bottom (Fig. 1 top left). In the off-state, the inductive posts are isolated, having almost no effect on the impedance of the SIW. In the on-state, the circular pads are connected to the top of the structure, and the shunt admittance of the SIW changes drastically, thus reflecting the incoming propagating wave.

### *B. Single-Pole Dual-Double-Throw Switch*

The design of the SPDDT switch uses an SIW coupler with four inductive posts and PIN diodes added similar to those in the SPST switch configuration, as shown in Fig. 2. Note that all ports are equipped with SIW-to-microstrip transitions which are bent to provide access for measurement equipment. The four inductive posts are placed in the junction of port 3, positioned with an angle of 20° which has been found to yield acceptable performance during parametric analysis.

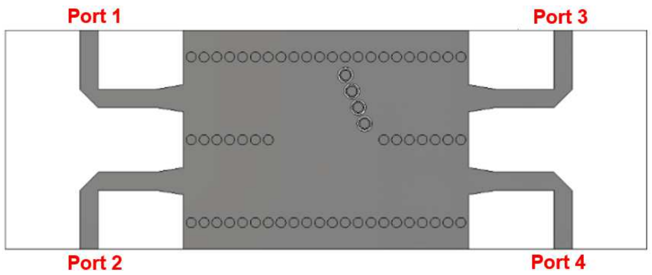


Fig. 2. SIW SPDDT switch design.

## III. RESULTS

Numerical characterizations were obtained through the commercial software CST Microwave Studio. All circuits are designed on a Rogers Duroid/RT 6002 dielectric substrate with relative permittivity of 2.94, loss tangent of 0.0012 at 10 GHz and height of 508 µm. The parameters' dimensions are presented in Table I.

TABLE I
PARAMETER DIMENSIONS OF THE PROPOSED CIRCUIT.

| Parameter | Value (mm) |
|---|---|
| $a_{SIW}$ | 5.80 |
| $d$ | 0.70 |
| $d_g$ | 1.10 |
| $g$ | 0.10 |
| $L_t$ | 1.90 |
| $p$ | 0.90 |
| $p_L$ | 1.20 |
| $W_{50}$ | 1.28 |
| $W_t$ | 1.89 |

Fig. 3 presents the result of the [S] parameters of the SIW (Fig. 1 bottom without posts). The simulation shows that insertion loss, $S_{21}$, is 0.9 dB and the return loss, $S_{11}$, is better than 15 dB.

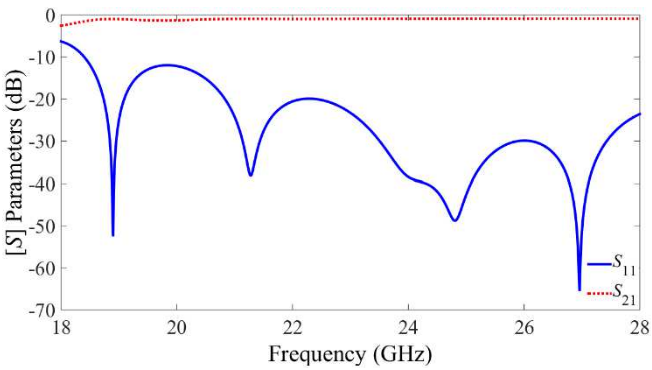


Fig. 3. Simulated $S$ parameters of the SIW with microstrip ports.

The number, spacing and size of the inductive posts are factors to be considered in switching performance. Fig. 4 compares $S$ parameters results for two different inductive posts' size, $d$ = 0.4 mm and $d$ = 0.7 mm, and same spacing $p_L$ = 1.2 mm, considering off- and on-states. In the off-state, the posts with $d$ = 0.4 mm show to have a better performance. In the on-state, the results for posts with $d$ = 0.7 mm present a good isolation, better than 15 dB from 18 to 25.17 GHz.

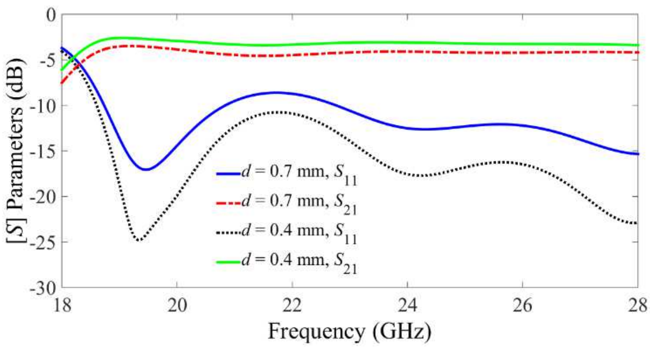


(a)

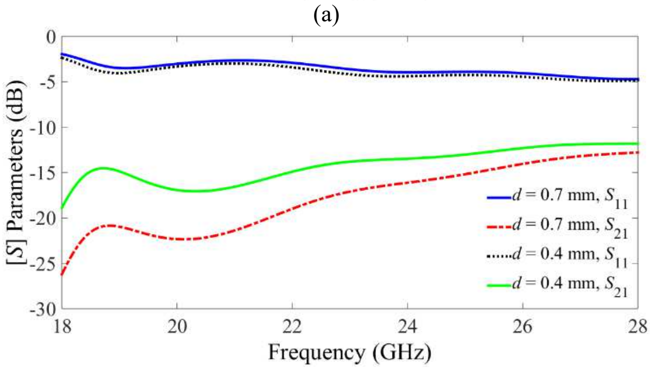


(b)

Fig. 4. Simulated $S$ parameters of the SIW SPST with different sizes of the posts for the (a) off-state and (b) on-state.

The performance of the SIW SPST switch with $d$ = 0.7 mm and different numbers of inductive posts and spacing, $p_L$ = 1.4 mm for 3 posts and $p_L$ = 1.2 mm for 4 posts, are presented in Fig. 5. In the off-state, the smaller number of posts at a given width has a slightly better insertion and return loss. In the on-state, the larger number of posts shows to have higher isolation. Comparing the number, size and spacing of the posts, four inductive posts with widths of 0.7 mm are employed for the design of the switch.

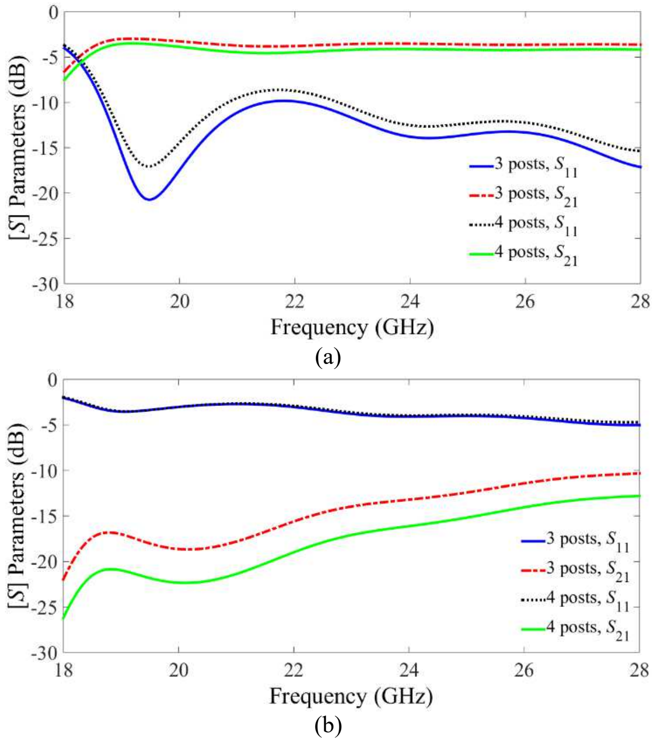


Fig. 5. Simulated $S$ parameters of the SIW SPST with different numbers of the posts for the (a) off-state and (b) on-state.

Fig. 6 shows the E-field distributions of the designed SIW SPST switch at 23 GHz considering the cases of (a) no posts, (b) off-state, and (c) on-state. Comparing the SIW SPST with no posts and off-state, it is observed that the off-state results resemble those of the traditional SIW. When we switch to the on-state, the incoming EM wave is almost completely reflected.

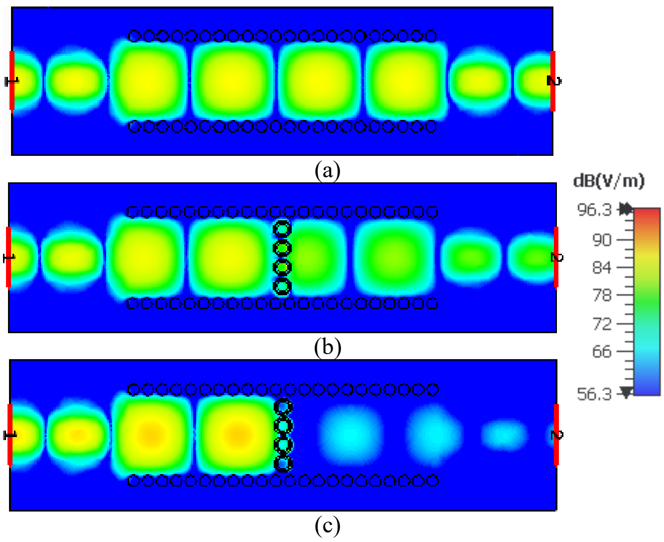


Fig. 6. E-field distributions at 23 GHz of the SIW SPST switch with (a) no posts, and with posts in (b) off-state and (c) on-state.

Fig. 7 demonstrates the performance of the SIW directional coupler (Fig. 2 without posts) simulated in CST Microwave Studio. Return loss and isolation are better than 10 dB between 18 and 25.9 GHz.

The simulated $S$ parameter results for the SIW SPDDT switch with port 1 excitation, considering off-state and on-state are presented in Fig. 8. In the off-state, return loss and

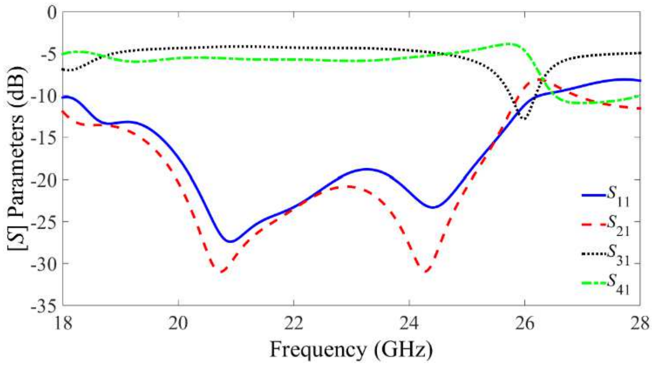


Fig. 7. Simulated $S$ parameters of the SIW coupler.

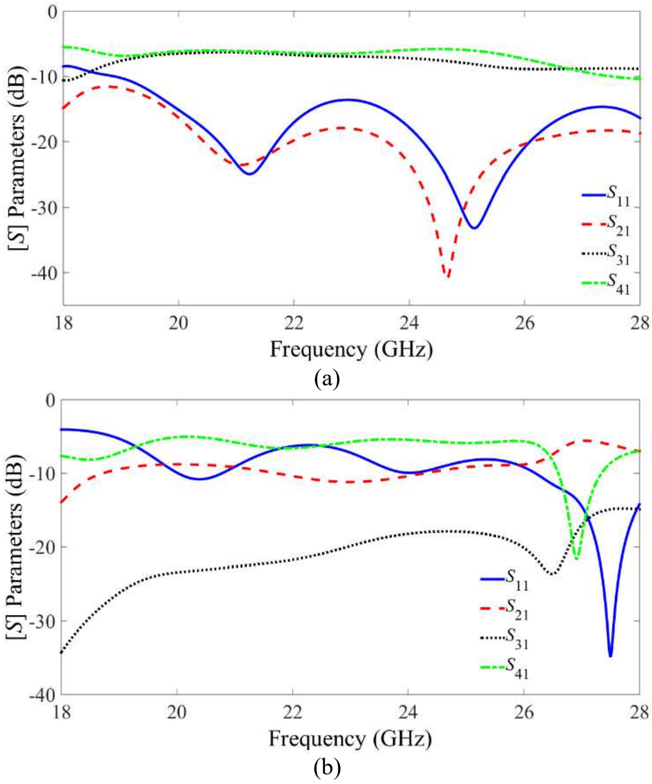


Fig. 8. Simulated $S$ parameters of the SIW SPDDT for the (a) off-state and (b) on-state.

isolation are greater than 10 dB, and the EM wave at port 1 propagates to port 3 and port 4, which are joint at -6 dB. In the on-state, the incident EM wave at port 1 propagates to port 2 and port 4, with the isolation in port 3 better than 15 dB from 18 to 27.4 GHz.

The E-field distributions of the designed SIW SPDDT switch/power divider at 23 GHz with port 1 excitation is presented in Fig. 9 for (a) off-state and (b) on-state. It can be observed, when switching from off-state to on-state, that the EM waves previously directed to ports 3 and 4 appear at ports 2 and 4 after activating the switch.

## IV. Conclusion

A K-band SIW single-pole dual-double-throw (SPDDT) switch is presented. This work is divided in four steps: first the design of the SIW was done and then, second, an analysis of the SIW SPST switch with different size, spacing and numbers of inductive posts was performed.

Third, an SIW coupler was designed and, fourth, inductive posts were placed in one of its junctions to get the final configuration of the SPDDT switch. In the off-state, the inductive posts have little influence on the impedance of the circuit, which allows the incident signal to be transmitted. In the on-state, the incident signal is reflected by the inductive posts, steering it towards another port. Simulations show that the proposed circuit exhibits good isolation, making it promising for promising for multiple-beam antenna and or 5G applications.

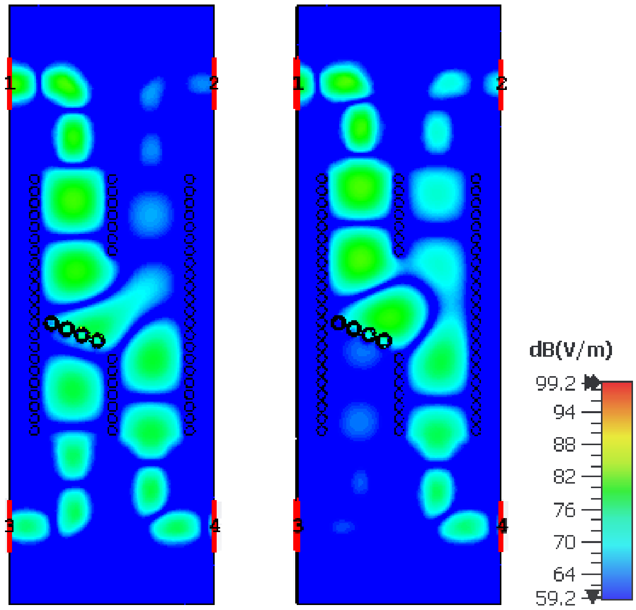


Fig. 9. E-field distributions at 23 GHz of the SIW SPDDT switch/power divider for (a) off-state and (b) on-state.

## REFERENCES


[1] R. Khan, A. A. Al-Hadi, P. J. Soh, M. R. Kamarudin, M. T. Ali and Owais, "User influence on mobile terminal antennas: A Review of challenges and potential solution for 5G antennas," *IEEE Access*, vol. 6, pp. 77695-77715, 2018, doi: 10.1109/ACCESS.2018.2883788.

[2] S. Kumar, A. S. Dixit, R. R. Malekar, H. D. Raut and L. K. Shevada, "Fifth generation antennas: A comprehensive review of design and performance enhancement techniques," *IEEE Access*, vol. 8, pp. 163568-163593, 2020, doi: 10.1109/ACCESS.2020.3020952.

[3] D. F. Mamedes, M. Esmaeili, and J. Bornemann, "K-band substrate integrated waveguide variable phase shifter," in *Proc. 10th Eur. Conf. Antennas Propag.* (*EuCAP*), 2016, pp. 1-4, doi: 10.1109/EuCAP.2016.7481602.

[4] Z. Kordiboroujeni and J. Bornemann, "Designing the width of substrate integrated waveguide structures," *IEEE Microw. Wireless Compon. Lett.*, vol. 23, no. 10, pp. 518-520, Oct. 2013, doi: 10.1109/LMWC.2013.2279098.

[5] A. Fathoni, N. Ismail, S. Risnanto, and A. Munir, "Design of compact SIW bandpass filter for GPS application," in *Proc. 14th Int. Conf. Telecomm. Systems, Services, Appl.* (*TSSA*), 2020, pp. 1-4, doi: 10.1109/TSSA51342.2020.9310869.

[6] Y. Liu, Q. Cheng, A. N. Khan, H. Giddens, M. M. Torrico, and Y. Hao, "Low-profile beam steerable patch array with SIW feeding network," *IEEE Access*, vol. 8, pp. 164178-164186, 2020, doi 10.1109/ACCESS.2020.3021744.

[7] S. Wei, C. Yang, Y. Chen, T. Chen, and C. Chang, "V- and W-band substrate integrated waveguide (SIW) mechanical switch," *IEEE Trans. Microw. Theory Tech.*, vol. 66, no. 6, pp. 3090-3098, June 2018, doi: 10.1109/TMTT.2018.2825381.

[8] A. Ghiotto, S. Adhikari, and K. Wu, "Ferrite-loaded substrate integrated waveguide switch," *IEEE Microw. Wireless Compon. Lett.*, vol. 22, no. 3, pp. 120-122, Mar. 2012, doi: 10.1109/LMWC.2012.2183859.

[9] H. Chen, W. Che, Y. Cao, W. Feng, and K. Sarabandi, "Function-reconfigurable between SPDT switch and power divider based on switchable HMSIW unit," *IEEE Microw. Wireless Compon. Lett.*, vol. 27, no. 3, pp. 275-277, Mar. 2017, doi: 10.1109/LMWC.2017.2662320.

[10] D. Deslandes, "Design equations for tapered microstrip-to-substrate integrated waveguide transitions," in *IEEE MTT-S Int. Microw. Symp. Dig.*, 2010, pp. 704-707, doi: 10.1109/MWSYM.2010.5517884.